


Petrogenesis of the Late Triassic Mengsong strongly peraluminous granites in the southeastern Tibetan Plateau: highly fractionated from crystal mush

Feng Cong , Fu-Yuan Wu , Wen-Chang Li , De-Feng He , Zai-Bo Sun , Xiao-Ming Huang , Zhi-Zhong Hu & Han Zhao

To cite this article: Feng Cong , Fu-Yuan Wu , Wen-Chang Li , De-Feng He , Zai-Bo Sun , Xiao-Ming Huang , Zhi-Zhong Hu & Han Zhao (2020): Petrogenesis of the Late Triassic Mengsong strongly peraluminous granites in the southeastern Tibetan Plateau: highly fractionated from crystal mush, International Geology Review, DOI: [10.1080/00206814.2020.1839975](https://doi.org/10.1080/00206814.2020.1839975)

To link to this article: <https://doi.org/10.1080/00206814.2020.1839975>

 View supplementary material [↗](#)

 Published online: 01 Nov 2020.

 Submit your article to this journal [↗](#)

 View related articles [↗](#)

 View Crossmark data [↗](#)

ARTICLE



Petrogenesis of the Late Triassic Mengsong strongly peraluminous granites in the southeastern Tibetan Plateau: highly fractionated from crystal mush

Feng Cong^{a,b}, Fu-Yuan Wu^a, Wen-Chang Li^b, De-Feng He^c, Zai-Bo Sun^d, Xiao-Ming Huang^b, Zhi-Zhong Hu^b and Han Zhao^a

^aState Key Laboratory of Lithospheric Evolution, Institute of Geology and Geophysics, Chinese Academy of Sciences, Beijing, China; ^bChengdu Center of China Geological Survey, Chengdu, China; ^cInstitute of Geochemistry, Chinese Academy of Sciences, Guiyang, China; ^dYunnan Institute of Geological Survey, Kunming, China

ABSTRACT

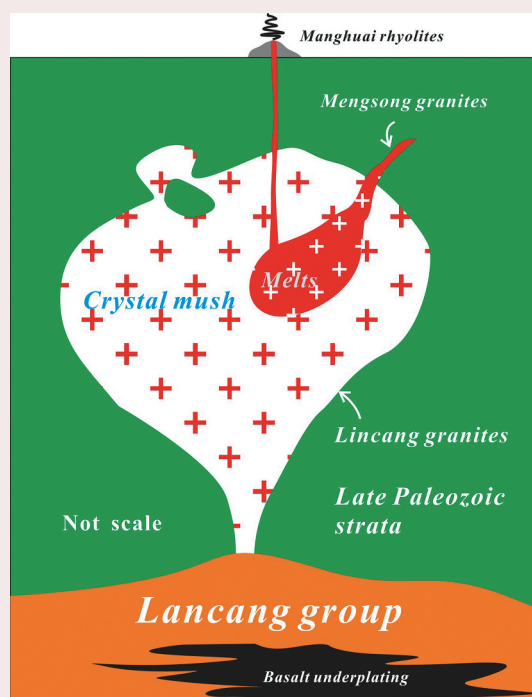
The Triassic Lincang granites make up the largest peraluminous granitic batholith in the Changning-Menglian Paleo-Tethys orogenic belt, southeastern Tibetan Plateau. It is undoubtedly very important to investigate the role of crustal magmatism in the evolution of the Changning-Menglian Paleo-Tethys orogenic belt. The Late Triassic Mengsong pluton is composed of strongly peraluminous two-mica monzogranites, and is located in the southernmost part of the Lincang batholith. Despite all being peraluminous granites, they differ markedly in dimensions, petrographic and geochemical characteristics. Mengsong two-mica monzogranites have low contents of TiO_2 , FeO^{tot} , MgO , and CaO , but high values of SiO_2 and Na_2O , compared to biotite monzogranites of the Lincang batholith. The Lincang biotite monzogranites show an enrichment in light rare earth elements (LREE) and weak Eu anomalies ($\delta\text{Eu} = 0.3\text{--}0.8$). However, the Mengsong two-mica monzogranites show a clear tetrad effect and contain pronounced negative Eu anomalies ($\delta\text{Eu} = 0.1\text{--}0.3$). Geochemical compositions and mineral textures of two-mica monzogranites indicate that they are of highly fractionated type affinity. The two-mica monzogranites are characterized by negative $\epsilon_{\text{Hf}}(t)$ values (-9.3 to -1.7) and $\epsilon_{\text{Nd}}(t)$ values (-9.6 to -7.9), while the biotite monzogranites have lower $\epsilon_{\text{Hf}}(t)$ values (-15.5 to -6.1) and $\epsilon_{\text{Nd}}(t)$ values (-14.5 to -11.5). Isotopic compositions suggest that they were cogenetic and derived from partial melting of the lower crust. Our petrogenetic and zircon U-Pb age data support models that relate the Lincang and Mengsong granites to post-collisional magmatism in the Changning-Menglian Paleo-Tethys orogenic belt during the Middle to Late Triassic. We interpret the Mengsong pluton to represent highly fractionated melts from crystal mush reservoirs and the Lincang granites to be complementary residual.



ARTICLE HISTORY


Received 22 May 2020
Accepted 17 October 2020

KEYWORDS

Mengsong pluton; Lincang batholith; strongly peraluminous; petrogenesis; crystal mush; post-collisional



CONTACT Feng Cong  673103623@qq.com  State Key Laboratory of Lithospheric Evolution, Institute of Geology and Geophysics, Chinese Academy of Sciences, Beijing, China

 Supplemental data for this article can be accessed [here](#).

© 2020 Informa UK Limited, trading as Taylor & Francis Group

1. Introduction

The geochemistry of granites have previously been interpreted using the I- and S-type classifications of Chappell and White (1992). They described the granites formed by igneous-sourced melt as 'I-type' and those formed from sedimentary-sourced melt as 'S-type'. In addition, according to the extent of magmatic differentiation, granite might be divided into cumulated and fractionated types (Chappell and Wyborn 2004; Wu *et al.* 2017). The Triassic Lincang granites make up the largest peraluminous granitic batholith in the southeastern Tibetan Plateau. It is widely believed that the Lincang granites are of S-type affinity, mainly supported by its peraluminous nature (Kong *et al.* 2012; Nie *et al.* 2012; Dong *et al.* 2013; Peng *et al.* 2013; Wang *et al.* 2014). However, based on their unfractionated geochemical signatures and cumulative textures, Cong *et al.* (2020) consider that the Lincang batholith exhibit typical features of cumulative granites. The Late Triassic Mengsong granites are strongly peraluminous and they are located in the southernmost part of the Lincang batholith (YBGMR 1980; Wang *et al.* 2015). Strongly peraluminous granite is a popular petrological term (Sylvester 1998; Chappell *et al.* 2012). This type of rock has an aluminous saturation index (ASI or A/CNK) ≥ 1.1 (Sylvester 1998). Several processes could explain the petrogenesis of the strongly peraluminous granites, including (a) fractional crystallization of metaluminous melts (Cawthorn *et al.* 1976; Zen 1986); (b) partial melting of peraluminous source rocks (Chappell *et al.* 2012); (c) alkali loss from end-stage volatile-bearing magmas (Martin and Bowden 1981); or (d) contamination of sedimentary country rocks (Ugidos and Recio 1993). Thus, the actual origin of the strongly peraluminous granites remains controversial. The two-mica monzogranites listed above occur in the Mengsong pluton, making it an ideal site to research the forming process of strongly peraluminous granites. In addition, the Late Triassic Mengsong two-mica monzogranites contain biotite (<5%) as the only mafic mineral. They have a high silica content (>74 wt. % SiO₂), but low contents of TiO₂, FeO^{tot}, MgO, CaO, and total REE, with a clear tetrad effect in REE patterns. Sn mineralization is also developed in the Mengsong two-mica monzogranites (YBGMR 1980). These features suggest that the Mengsong pluton underwent significantly fractional crystallization. However, the exact mechanism for fractional crystallization is still unknown. Furthermore, the relationship between the unfractionated Lincang batholith and fractionated Mengsong pluton is still unclear, that restrict our understanding of the crustal generation of the Changning-Menglian Paleo-Tethys orogenic belt. Here we present combined zircon U-Pb geochronology and Lu-Hf isotopes, whole-rock elements, and Nd isotopes to investigate the mechanism for fractional

crystallization, and then to constrain the petrogenesis of the Mengsong pluton.

2. Geological setting and samples

Mainland southeastern Asia comprises a complex assembly of continental blocks, arc terranes, and suture zones and accreted continental crust (Metcalf 2011). The two major continental masses within Mainland southeastern Asia are the Indochina and Sibumasu Terranes. They collided with each other and caused the Indosinian orogeny during the Late Permian–Early Triassic after the prolonged subduction of the Paleo-Tethys Ocean, represented by the Changning-Menglian suture in the southeastern Tibetan Plateau, the Chiang Rai suture in Thailand, and the Bentong-Raub suture in Peninsular Malaysia (Sone and Metcalfe 2008; Metcalfe 2011; Gardiner *et al.* 2016). The Changning-Menglian suture contains ophiolitic mélanges, volcanics, shallow-marine carbonates, and deep-sea sedimentary rocks with substantial pelagic cherts, and is unconformably overlain by Triassic units (Zhong 1998; Sone and Metcalfe 2008).

The Main Range Province of the southeastern Asian Triassic granite belt extends from Lincang in the southeastern Tibetan Plateau and eastern Myanmar through Chiang Rai in Thailand, and south to Peninsular Malaysia (Hutchison 1977; Mitchell 1977; Cobbing *et al.* 1986; Charusiri *et al.* 1993; Gardiner *et al.* 2016). The Lincang batholith is located to the east of the Changning-Menglian Paleo-Tethys suture in the southeastern Tibetan Plateau. During recent years, the Lincang batholith is hotly studied to decipher the evolution of the Paleo-Tethys (Zhong 1998; Hennig *et al.* 2009; Kong *et al.* 2012; Nie *et al.* 2012; Dong *et al.* 2013; Peng *et al.* 2013; Wang *et al.* 2014, 2015; Deng *et al.* 2018). The Lincang granites are a composite batholith of predominately alkali-feldspar megacrystic medium to coarse-grained biotite monzogranites with subordinate granodiorites (Li 1996), and have zircon U-Pb ages that mainly range from Middle to Late Triassic (Hennig *et al.* 2009; Dong *et al.* 2013; Peng *et al.* 2013; Wang *et al.* 2015; Cong *et al.* 2020). The Lincang batholith is elongated in the N-S direction, occurring as a 'Z' shape in the southeastern Tibetan Plateau, and cover an area of 7400 km² (Figure 1(b)). The batholith has a length of 370 km and a width of 10–50 km, and extends from Jinghong to Lincang in the Yunnan Province of China (Li 1996). To the east, the Lincang batholith is bordered by the Lancangjiang zone, which contains basaltic andesites and gabbros, and hosts small granodiorite intrusions of Permian age (Hennig *et al.* 2009) shown as mafic complex in Figure 1(b). This zone marks the boundary between the Lincang batholith and the Lanping-Simao block, the presumed northern extension of Indochina (Dong *et al.* 2013). The

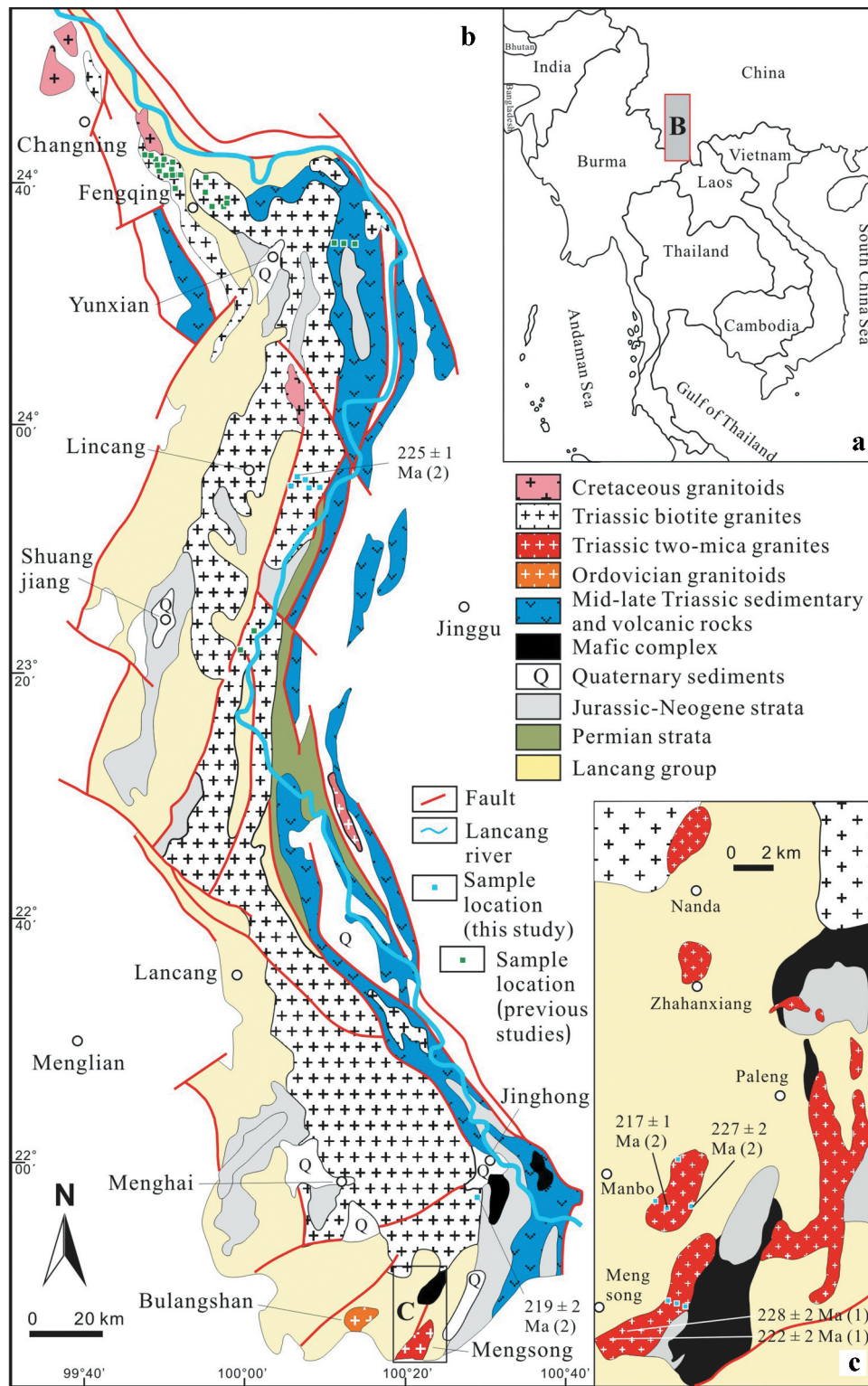


Figure 1. (a) and (b) Simplified geological map of the Lincang batholith in the southeastern Tibetan Plateau (after YBGM 1990; Dong *et al.* 2013; Wang *et al.* 2017). (c) Simplified geological map and sample locations of the Mengsong pluton (after YBGM 1980). The zircon U-Pb ages of the granites are from ¹Wang *et al.* (2015) and ²this study.

Lincang batholith is bordered to the west by the Changning-Menglian suture. The Lincang granite is overlain by unconformities composed of the terrestrial red-beds of

Mid-Jurassic volcano-sedimentary rocks. There are also several Precambrian crustal rocks, known as the Lancang group (Figure 1(b)). Zhong (1998) considered the Lancang

group to be composed of Meso-/Neo-Proterozoic meta-volcanic and metasedimentary rocks. Moreover, Zhang *et al.* (1993) indicated that the Lancang group had the characteristics of a subduction mélangé, highlighting its tectonic significance. The Triassic volcanic rocks of the Manghuai, Xiaodingxi, and Manghuihe formations are exposed parallel to the eastern margin of the Lincang batholith (Wang *et al.* 2010; Peng *et al.* 2013) (Figure 1(b)). The eastern margin of the volcanic rocks is delimited by a major mylonitic fault zone within the Triassic-Jurassic strata of the Lanping-Simao basin (Figure 1(b)). The Late Cretaceous granitoids are located at the Xinjie and Luyintang, north of the Lincang batholith. The Ordovician granitoids were also identified at Bulangshan (Sun *et al.* 2018), south of the Lincang batholith (Figure 1(b)).

Representative rock types were selected from the Mengsong pluton and Lincang batholith for geochemical studies (Figure 1(b,c)). The Mengsong pluton (Figure 2(e–g)) is located about 40 km southwest of Jinghong city, Yunnan Province. It is exposed as five stocks of a few km² in the S–N direction, as Mengsong, Manbo, Paleng, Zhahanxiang, and Nada, respectively (Figure 1(c)) (YBGMR 1980). They were intruded into the Lancang group and Permian mafic rocks (Figure 1(c)). The Nada stock display gradational contact with the Lincang biotite monzogranites (Figure 1(c)). The Mengsong pluton is mainly composed of fine- to medium-grained two-mica monzogranites, which mainly consist of quartz, alkali-feldspar, plagioclase, muscovite, and biotite (Figure 2(a–c)). Alkali-feldspar is predominantly microcline (Figure 2(a)), with a small amount of orthoclase. The accessory minerals consist of apatite, zircon, and rare opaque minerals. The Lincang biotite monzogranites were collected from east of Lincang city (Figure 1(b)) and mainly consist of quartz, plagioclase, alkali-feldspar, and biotite (Figure 2(d,h)). The accessory minerals consist of apatite, zircon, monazite, and rare magnetite. The detailed lithological characteristics of the analytical samples are shown in Supp. Table 1. In the QAP diagram (Figure 3), they plot in the monzogranite fields.

3. Analytical methods

Whole rock major and trace elements were analysed at the Institute of Geochemistry, the Chinese Academy of Sciences. Major elements were determined using an X-ray fluorescence spectrometer (XRF). Analytical uncertainties were 3% for major elements. Trace element analyses were performed on a Finnigan MAT ELEMENT inductively coupled plasma mass spectrometer (ICP-MS).

Analytical uncertainties were 5% for trace elements with concentrations ≥ 20 ppm and 10% for those < 20 ppm.

The U-Pb analyses of zircon were conducted by LA-ICP-MS at the Wuhan Sample Solution Analytical Technology Co., Ltd., Wuhan, China. Laser sampling was performed using a GeolasPro laser ablation system that consists of a COMPexPro 102 ArF excimer laser (wavelength of 193 nm and maximum energy of 200 mJ) and a MicroLas optical system. An Agilent 7700e ICP-MS instrument was used to acquire ion-signal intensities. Helium was applied as a carrier gas. Argon was used as the make-up gas and mixed with the carrier gas via a T-connector before entering the ICP. The laser spot diameter and frequency were set to 30 μm and 10 Hz in this study. Zircon 91,500 was used as the external standard, zircon GJ-1 was analysed as an unknown to monitor the data quality, and silicate glass NIST 610 was used to optimize the instrument. An Excel-based software, ICPMSDataCal, was used to perform off-line selection and integration of background and analysed signals, time-drift correction, and quantitative calibration for trace element analysis and U-Pb dating (Liu *et al.* 2008).

Sm-Nd isotopic compositions of whole-rock powders were performed at the Laboratory for Radiogenic Isotope Geochemistry, University of Science and Technology of China. About 150 mg of sample powder was dissolved in a mixture of HClO₄ and HF acid solution at 120°C for seven days. The solution was dried and re-dissolved in HCl acid solution. Sm-Nd isotopic ratios were measured on a Finnigan MAT-262 spectrometer. Analytical precisions are stated as two-sigma standard errors and more details of the analytical technique are given in Chen *et al.* (2007).

Hafnium isotopic determination was performed on a Neptune multi-collector ICP-MS equipped with a Geolas-193 laser ablation system (LA-MC-ICP-MS) at the Institute of Geology and Geophysics, Chinese Academy of Sciences. The analytical procedure described by Wu *et al.* (2006) was followed. During analyses, spot sizes of 50 μm , with a laser repetition rate of 8 Hz at 100 mJ, were used. The ¹⁷⁶Hf/¹⁷⁷Hf ratios of the zircon standard (GJ-1) were 0.281998 ± 0.000003 (2 σ , n = 234), similar to the ¹⁷⁶Hf/¹⁷⁷Hf ratios of 0.282000 ± 0.000005 (2 σ) recommended by Morel *et al.* (2008).

4. Results

4.1. U-Pb age

LA-ICP-MS zircon U-Pb isotopic data from 2 two-mica monzogranites from the Mengsong pluton and two biotite monzogranites from the Lincang batholith are shown in Supp. Table 2. Zircons from the biotite monzogranite

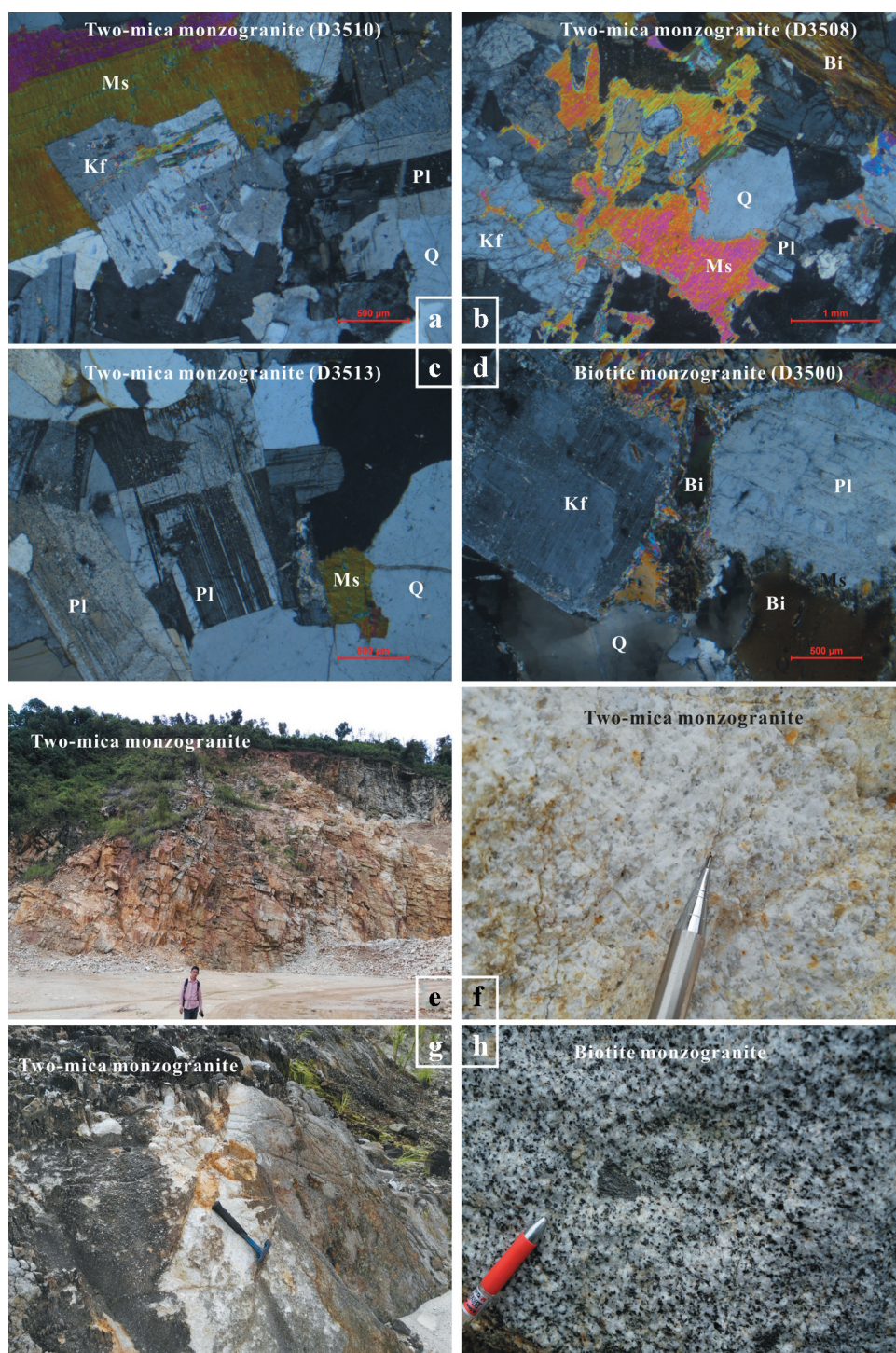


Figure 2. Textural and petrographic features of the Lincang and Mengsong granites in the southeastern Tibetan Plateau. (a), (b), (c), (e), (f) and (g) The Mengsong two-mica monzogranite consists mainly of quartz, alkali-feldspar, plagioclase, muscovite, and biotite. (d) and (h) The Lincang biotite monzogranite is made up of alkali-feldspar, plagioclase, quartz, and biotite. Mineral abbreviations: Kf = alkali-feldspar; Pl = Plagioclase; Q = Quartz; Bi = Biotite; Ms = Muscovite.

and two-mica monzogranites are mostly euhedral, up to 50–200 μm long, and have aspect ratios between 2:1 and 3:1. Oscillatory zoning is common in most crystals. Core-rim textures are observed within a few zircon grains. Most of the zircons are magmatic in origin.

Twenty-one analyses were obtained from 21 zircons of the biotite monzogranite (sample D3004) from the Lincang batholith. The zircons have variable abundances of Th (97–402 ppm) and U (307–1805 ppm). Th/U ratios vary between 0.14 and 0.71. Twenty-one analyses

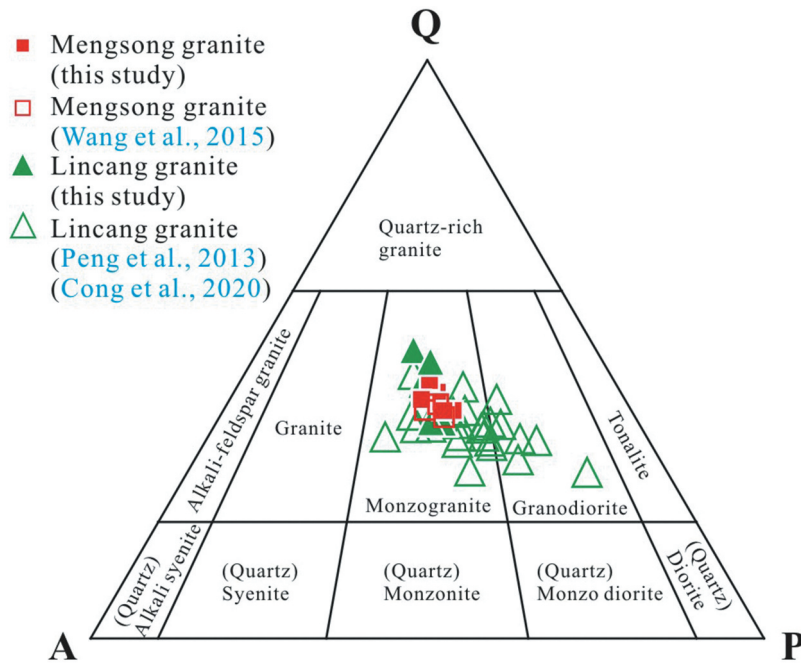


Figure 3. QAP classification of the Lincang and Mengsong granites from the southeastern Tibetan Plateau. The Mengsong granites plot in the monzogranite fields whereas the Lincang granites plot in the monzogranite and granodiorite fields.

produced a weighted mean $^{206}\text{Pb}/^{238}\text{U}$ age of 218.2 ± 1.4 Ma (Figure 4; MSWD = 1.7, 2σ), which is interpreted as the crystallization age of sample D3004. Spot 21 yielded significantly higher $^{206}\text{Pb}/^{238}\text{U}$ ages of 380 Ma, which is interpreted to have been obtained from a xenocryst.

Twenty-three analyses were obtained from 23 zircons in the biotite monzogranite (sample D3506) of the Lincang batholith. The zircons have variable abundance of Th (89–1177 ppm) and U (234–1840 ppm). The Th/U ratios are, therefore, variable, ranging from 0.08 to 0.87. Sixteen analyses produced a weighted mean $^{206}\text{Pb}/^{238}\text{U}$ age of 225.4 ± 1.1 Ma (Figure 4; MSWD = 1.1, 2σ), which is interpreted as the crystallization age of sample D3506. Spots 1, 5, 7, 13, 15, 22, and 23 yielded significantly higher $^{206}\text{Pb}/^{238}\text{U}$ ages of ca. 643, 469, 481, 450, 537, 917, and 939 Ma, respectively. The older ages are interpreted to have been obtained from relict zircons.

Seventeen analyses were obtained from 17 zircons in the two-mica monzogranite (sample D3511) from the Mengsong pluton. The zircons have variable abundance of Th (82–304 ppm) and U (188–1451 ppm). Th/U ratios vary between 0.13 and 0.63. Thirteen analyses produced a weighted mean $^{206}\text{Pb}/^{238}\text{U}$ age of 227 ± 2.0 Ma (Figure 4; MSWD = 1.9, 2σ), which is interpreted as the crystallization age of sample D3511. Spots 3, 6, 10, and 13 yielded significantly higher $^{206}\text{Pb}/^{238}\text{U}$ ages of ca. 447, 273, 251, and 515 Ma, respectively. The older ages are interpreted to have been obtained from xenocrysts.

Fourteen analyses were obtained from 14 zircons in the two-mica monzogranite (sample D3512) of the Mengsong pluton. The zircons have variable abundance of Th (105–2607 ppm) and U (193–6586 ppm). Th/U ratios vary between 0.08 and 0.87. Eleven analyses produced a weighted mean $^{206}\text{Pb}/^{238}\text{U}$ age of 217.3 ± 1.1 Ma (Figure 4; MSWD = 1.1, 2σ), which is interpreted as the crystallization age of sample D3512. Spots 12, 13, and 14 yielded significantly higher $^{206}\text{Pb}/^{238}\text{U}$ ages of ca. 241, 246, and 465 Ma, respectively. The older ages are interpreted to have been obtained from xenocrysts.

Overall, our zircon U-Pb dating results indicate that the Mengsong pluton and Lincang batholith are cogenetic with each other, and were emplaced around 217–227 Ma.

4.2. Major and trace elements composition

The results of the geochemical analyses are shown in Supp. Table 3. The biotite monzogranites have high contents of TiO_2 , FeO^{tot} , MgO, and CaO but low values of SiO_2 , compared to those of the two-mica monzogranites (Figure 5). While the two-mica monzogranites are characterized by high contents of SiO_2 (74.47–75.87%) and total alkalis ($\text{K}_2\text{O} + \text{Na}_2\text{O}$; 7.36–8.05%, $\text{K}_2\text{O} = 4.22\text{--}4.82\%$ and $\text{Na}_2\text{O} = 3.04\text{--}3.77\%$) but very low contents of TiO_2 (0.02–0.04%), FeO^{tot} (0.7–1.05%), MgO (0.03–0.09%), and CaO (0.1–0.33%). In general, as the silica contents increase in the Lincang granites, FeO^{tot} , CaO, MgO, TiO_2 and δEu decrease, while a poor correlation is observed with respect to K_2O and

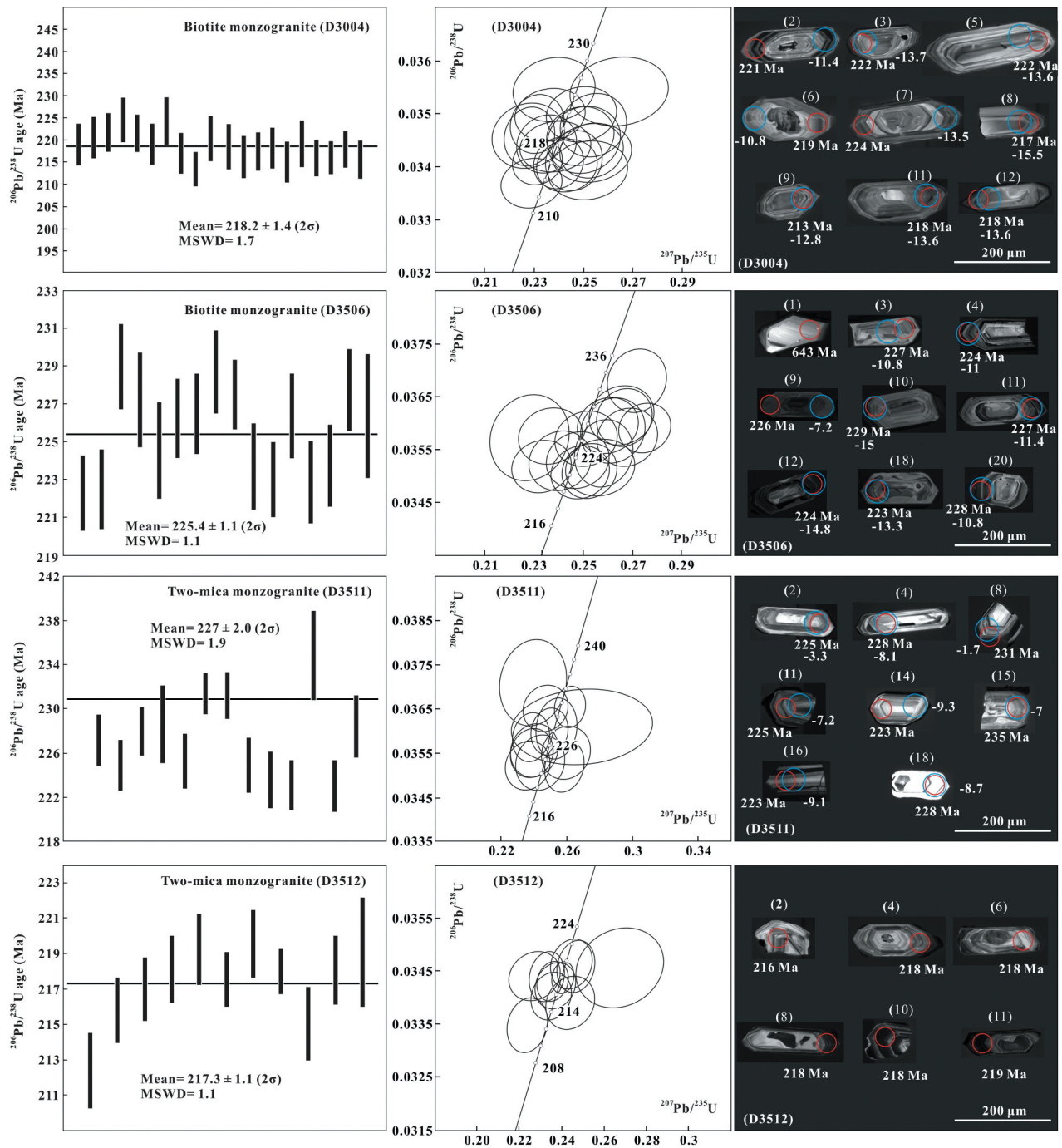


Figure 4. U-Pb isotopic analyses and Cathodoluminescence (CL) images of zircons in the Lincang and Mengsong granites from the southeastern Tibetan Plateau, showing $^{206}\text{Pb}/^{238}\text{U}$ ages and $\epsilon_{\text{Hf}}(t)$ values of analysed zircons. Red circle: analytical spot of U-Pb isotope; Blue circle: analytical spot of Hf isotope. The results indicate that the Mengsong granites were formed between 217–227 Ma.

Na_2O (Figure 5). All the studied granites have A/CNK ratios greater than 1.1 and plot in the strongly peraluminous field of the A/NK vs. A/CNK diagram (Figure 6(a)).

Chondrite-normalized REE patterns and primitive mantle-normalized trace element spidergrams are shown in Figure 7. The biotite monzogranites have a range of total REE (ΣREE) concentrations between 133 and 248 ppm. However, the two-mica monzogranites have very low

total REE (ΣREE) concentrations between 22 and 35 ppm. Chondrite-normalized REE patterns of the biotite monzogranites invariably show LREE enrichments with $(\text{La}/\text{Yb})_{\text{N}}$ ratios of 5.9 to 21.4 and negative Eu anomalies ($\delta\text{Eu} = 0.3\text{--}0.8$). However, the two-mica monzogranites show more variation, being characterized by nearly flat REE patterns ($(\text{La}/\text{Yb})_{\text{N}} = 1.3\text{--}1.7$) with a clear tetrad effect and pronounced Eu negative anomalies ($\delta\text{Eu} = 0.1\text{--}0.3$).

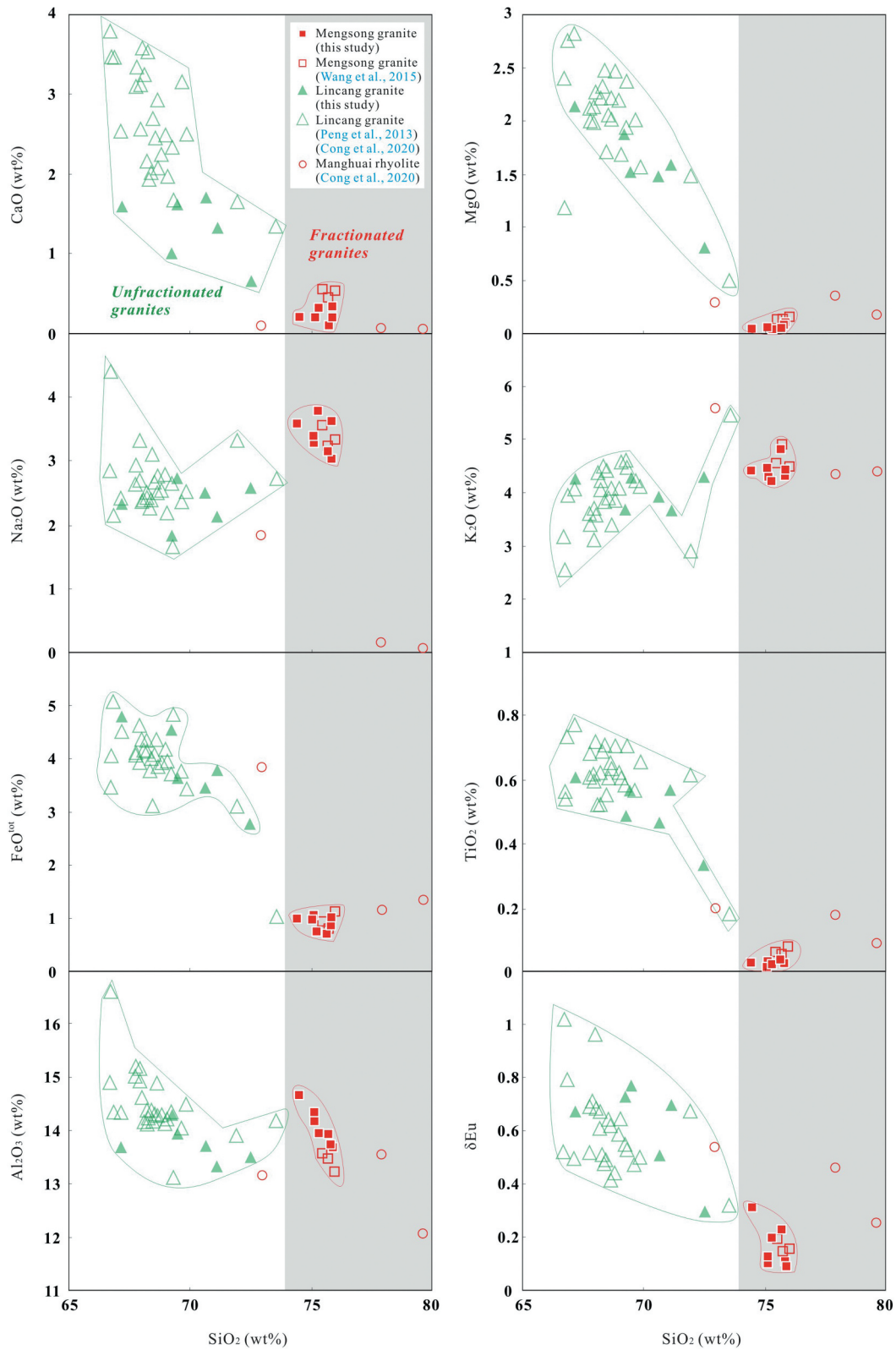


Figure 5. Harker diagrams for the Lincang and Mengsong granites in the southeastern Tibetan Plateau. The contents of MgO, CaO, FeO^{tot}, TiO₂, and δEu exhibited decreasing trends as SiO₂ increased from the Lincang granites to the Mengsong granites, which are identified as unfractionated and fractionated granites, respectively. A poor correlation is observed with respect to Na₂O and K₂O. The previous studies of the Mengsong granites and Manghuai rhyolites are from Wang *et al.* (2015) and Cong *et al.* (2020), respectively. The previous studies of the Lincang granites are from Peng *et al.* (2013) and Cong *et al.* (2020).

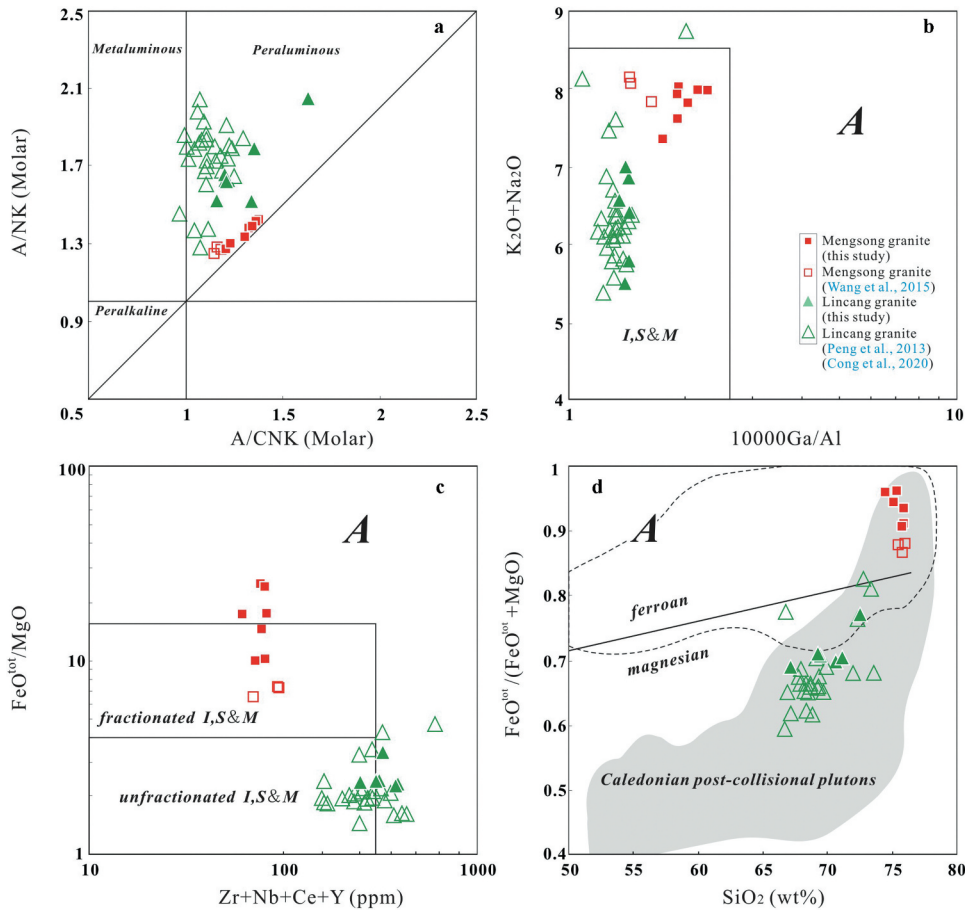


Figure 6. (a) A/NK vs. A/CNK plot showing the peraluminous nature of the Lincang and Mengsong granites from the southeastern Tibetan Plateau. A = Al₂O₃, N = Na₂O, K = K₂O, C = CaO (all in molar proportion). (b) (K₂O + Na₂O) vs. 10000 Ga/Al classification and (c) FeO^{tot}/MgO vs. (Zr + Nb + Ce + Y) classification diagrams (Whalen *et al.* 1987), indicating that the Lincang granites and Mengsong granites are unfractionated and fractionated I-, S-, and M-types, respectively. FG: Fractionated felsic granites; OGT: unfractionated M-, I- and S-type granites. (d) FeO^{tot}/(FeO^{tot} + MgO) vs. SiO₂ diagram (Frost *et al.* 2001), indicating that the Lincang and Mengsong granites are magnesian and ferroan granitoids, respectively. They are similar to the Caledonian post-collisional plutons. Data sources: (1) Lincang granites: Dong *et al.* (2013), Cong *et al.* (2020); this study; (2) Mengsong granites: Wang *et al.* (2015); this study.

The term ‘tetrad effect’ refers to the subdivision of the 15 lanthanide elements into four groups in a chondrite-normalized distribution pattern (Jahn *et al.* 2001). Despite the two-mica monzogranites having lower element contents than the biotite monzogranites (Supp. Table 3), their spidergrams show some similarities with characteristic negative anomalies in Ba, Nb, Sr, and Ti, and a positive anomaly in Pb (Figure 7). Zircon saturation thermometry (Watson and Harrison 1983) was applied to estimate the temperatures of the granitic melts. The biotite monzogranites exhibit higher temperatures of $T_{Zr} = 790\text{--}856\text{ }^{\circ}\text{C}$, while the two-mica monzogranites have significantly lower temperatures ($T_{Zr} = 663\text{--}692\text{ }^{\circ}\text{C}$) (Figure 10(a)).

4.3. Nd-Hf isotope data

It should be noted that the Sr isotopic data for the Mengsong two-mica monzogranites have limited

applicability because these samples have high Rb/Sr ratios (63–293), resulting in imprecise initial $^{87}\text{Sr}/^{86}\text{Sr}$ ratio calculations. The results of the Nd isotopic analyses are shown in Supp. Table 4. The Lincang granites have $^{143}\text{Nd}/^{144}\text{Nd}$ ratios of 0.511800 to 0.511951 and a variety of $\epsilon_{Nd}(t=220\text{ Ma})$ values that range from -14.5 to -11.5 , corresponding to T_{DM2} (two-stage model ages) ages of 1924–2167 Ma. The Mengsong granites have $^{143}\text{Nd}/^{144}\text{Nd}$ ratios of 0.512198 to 0.512268 and $\epsilon_{Nd}(t=220\text{ Ma})$ values that range from -9.6 to -7.9 , corresponding to T_{DM2} ages of 1635–1779 Ma. The Mengsong granitic pluton has slightly higher $\epsilon_{Nd}(t)$ values than those of the Lincang batholith in this study.

In-situ magmatic zircon Hf isotope data from biotite monzogranites of the Lincang batholith and two-mica monzogranites of the Mengsong pluton are shown in Supp. Table 5. Twenty analyses for sample D3004 produced $^{176}\text{Hf}/^{177}\text{Hf}$ values of 0.282212 ± 0.000017 (2σ) to 0.282347 ± 0.000019 (2σ). The $\epsilon_{Hf}(t)$ values of zircon,

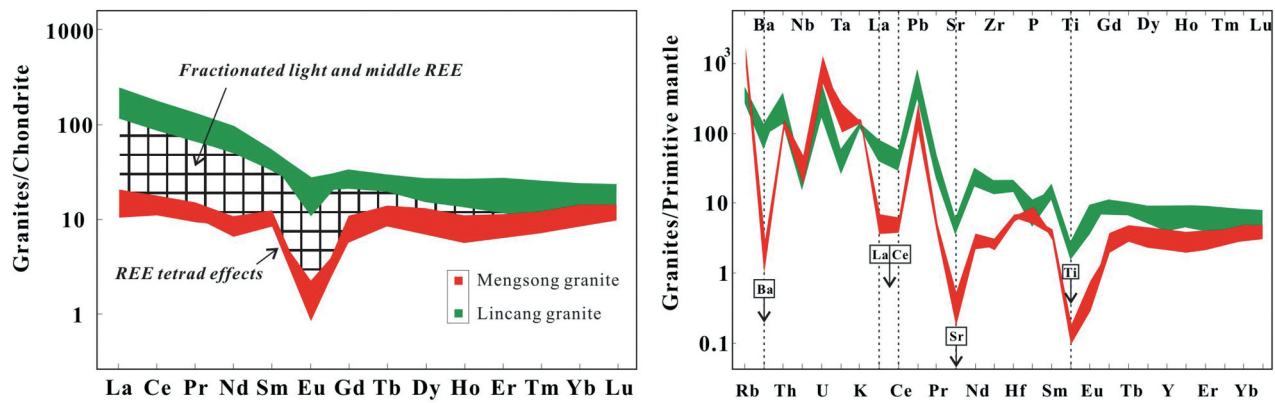


Figure 7. (a) Chondrite-normalized REE patterns and (b) primitive mantle normalized trace element patterns of the Lincang and Mengsong granites from the southeastern Tibetan Plateau. Chondrite and primitive mantle values are from Sun and McDonough (1989).

when calculated for their U-Pb ages, range from -15.5 to -10.8 (Figure 9), corresponding to T_{DM2} ages of 1912–2211 Ma. Sixteen spot analyses were collected from sample D3506. The measured $^{176}\text{Hf}/^{177}\text{Hf}$ values range from 0.282222 ± 0.000017 (2σ) to 0.282475 ± 0.000019 (2σ). The $\epsilon_{\text{Hf}}(t)$ values of zircon, when calculated back to their U-Pb ages, range from -15 to -6.1 (Figure 9), corresponding to T_{DM2} ages of 1622–2188 Ma. Thirteen spot analyses were collected from sample D3511, resulting in $^{176}\text{Hf}/^{177}\text{Hf}$ values that range from 0.282389 ± 0.000021 (2σ) to 0.282601 ± 0.000028 (2σ). The $\epsilon_{\text{Hf}}(t)$ values of zircon, when calculated back to their U-Pb ages, range from -9.3 to -1.7 (Figure 9), corresponding to T_{DM2} ages of 1342–1825 Ma. The Mengsong granitic pluton has higher $\epsilon_{\text{Hf}}(t)$ values than those of the Lincang batholith. In summary, all samples of the Late Triassic intrusions show variably negative $\epsilon_{\text{Nd}}(t)$ and $\epsilon_{\text{Hf}}(t)$ values.

5. Discussion

5.1. Highly fractionated type of Mengsong granites

The Lincang and Mengsong granites are closely related spatially and temporally in the Changning-Menglian Paleo-Tethys orogenic belt (YBGMR 1990). Spatially, the Mengsong granitic pluton display gradational contact with Lincang batholith. Both of them were emplaced into the Lancang group (Figure 1(b)). Wang *et al.* (2015) reported zircon U-Pb ages of 222 Ma and 228 Ma on Mengsong granites. Thus, previous and our geochronological studies suggest that the Mengsong granitic pluton was emplaced around 217–228 Ma (Wang *et al.* 2015 and this study). Our new U-Pb zircon ages of 218 Ma and 225 Ma from the Lincang biotite monzogranites are consistent with the 203–235 Ma age range typical of the Lincang batholith (Fan *et al.* 2009; Hennig *et al.* 2009; Jian *et al.* 2009; Kong *et al.* 2012; Nie *et al.* 2012; Peng *et al.* 2006, 2013; Dong *et al.*

2013; Wang *et al.* 2014). In the Changning-Menglian Paleo-Tethys orogenic belt, the Lincang batholith is paralleled by the Manghuai rhyolites, which exhibit an age range of 229–234 Ma (Peng *et al.* 2013). Therefore, the Mengsong granitic pluton, Lincang batholith and Manghuai rhyolites are cogenetic with each other in the Changning-Menglian Paleo-Tethys orogenic belt.

Granitic rocks have commonly been divided into I-, S-, M-, and A-types according to their protolith nature (Pitcher 1982). Moreover, according to the extent of magmatic differentiation, granite might be divided into cumulated and fractionated types (Chappell and Wyborn 2004; Wu *et al.* 2017). Microcline is the most common species of potassium feldspar in highly fractionated granite (Wu *et al.* 2017) and it is common in the two-mica monzogranites of this study (Figure 2(a)). In addition, Mengsong two-mica monzogranites contain biotite (<5%) as the only mafic mineral, while the Lincang batholith is mostly biotite-bearing monzogranites. Furthermore, Sn mineralization is developed in the Mengsong two-mica monzogranites (YBGMR 1980). Generally, rare-metal mineralization is an important evidence of highly fractionated granite (Wu *et al.* 2020). Hence, mineralogical features indicate that fractional crystallization took place during the formation of the two-mica monzogranites. Geochemically, the two-mica monzogranites are high-silica (generally >74 wt%) rocks, with very low contents of TiO_2 , FeO^{tot} , MgO, and CaO (Figure 5) and strong light and middle REE, Eu, Ba, Sr, and Ti depletion (Figure 7), indicating fractionation in the generation of these rocks. The low content of TiO_2 , FeO^{tot} , MgO, and CaO suggests that fractionation of biotite was likely to have played a role in the evolving magmatic systems. Strong Eu depletion requires extensive fractionation of plagioclase (Wu *et al.* 2003). Furthermore, the biotite monzogranites have higher Sr (75–130 ppm) and Ba (415–977 ppm) concentrations, while the two-mica monzogranites of Mengsong have significantly lower Sr (3.7–11.1

ppm) and Ba (7.6–19.8 ppm) concentrations in the plot of Ba vs. Sr (Figure 10(d)). This is explained by fractionation of alkali-feldspar, or plagioclase and biotite together. Sr was selected to compare with Rb in Figure 11. From the biotite monzogranites to two-mica monzogranites, the Sr contents decrease by up to two orders of magnitude with increasing Rb contents. The high Rb/Sr ratios (63–293) observed in the two-mica monzogranites suggest that they are highly fractionated rocks with the fractionation of plagioclase. The extreme enrichments in Rb and K is consistent with alkali-feldspar representing a late crystallizing phase in granitoids and that it does not participate in crystal-melt segregation (Glazner and Johnson 2013). Thus, fractionation of plagioclase, rather than alkali-feldspar, was the main reason for the change in Rb, Sr, Ba, and Eu contents of these rocks. The biotite monzogranites have nearly chondritic Zr/Hf ratios of 33.4–37.1. Notably, these ratios in the two-mica monzogranites ($Zr/Hf = 14\text{--}17.5$, $Nb/Ta = 2.4\text{--}3.2$) are significantly lower than chondritic values (Figure 10(b)). It is also shown that Zr/Hf ratios and T_{Zr} decrease synchronously from the biotite monzogranites to the two-mica monzogranites (Figure 10(a)). These features are considered an important indicator of magma evolution with fractional crystallization of zircon (Wu *et al.* 2017). Furthermore, highly fractionated granite often exhibits REE tetrad effects (Jahn *et al.* 2001) and the two-mica monzogranites investigated here share this feature (Figure 7). In addition to major phases, the variation of REE was mainly achieved by fractionation of apatite, monazite and allanite (Wu *et al.* 2003). Thus, the lower $(La/Yb)_N$ ratios (1.3–1.7) of two-mica monzogranites just infer there might be monazites, allanite and apatite fractional crystallization in the granitic system. The low total REE (22–35 ppm) and P_2O_5 (0.11–0.19%) contents of the two-mica monzogranites further support this observation. In a diagram of $(La/Yb)_N$ vs. La (Figure 10(c)), the variation in REE contents from biotite monzogranites to two-mica monzogranites seems to be consistent with fractionation of allanite and monazite. All of the aforementioned geochemical features indicate the separation of biotite, plagioclase, zircon, monazite, apatite, and allanite during magmatic evolution.

Geochemically, the Lincang batholith is characterized by low ratios of FeO^{tot}/MgO (1.84–3.42) in this study, indicating unfractionated features (Figure 6(c)). Harker diagrams (Figure 5) show that the contents of MgO , CaO , FeO^{tot} , TiO_2 , and δEu exhibited decreasing trends as SiO_2 increased from the biotite monzogranites to the two-mica monzogranites. These evolutionary trends in the composition of granites indicate that the biotite monzogranites are complementary residual of the two-mica monzogranites. In Figure 11, the biotite monzogranites can be interpreted as unfractionated rocks with low Rb/Sr ratios (1.7–3.9), which span the compositional spectrum of the Lincang granites of

a previous study (Peng *et al.* 2013; Cong *et al.* 2020). Accumulation of plagioclase and alkali-feldspar was the main reason for the change in mineral association and geochemical composition of these rocks. Enrichment of Ce (30.2–60.6 ppm) in the Lincang granites is evident in the plots of Whalen *et al.* (1987) (Figure 6(c)), in which it appears that some Lincang granitoids fall into the A-type field. High contents of Ce to this degree are similar to the Malaysian granitoids (Ng *et al.* 2015).

5.2. Origin of the strongly peraluminous Mengsong granites

Presently, the origin of strongly peraluminous granites is debated. Chappell *et al.* (2012) suggested that the high A/CNK ratio is an intrinsic feature of the sedimentary source and, thus, an important sign of an S-type granite. However, peraluminous granites can be produced either by partial melting of metasedimentary rocks or metaigneous rocks, which has been well documented by experimental petrology (Patiño 1999; Clemens and Stevens 2012). In addition, Cawthorn *et al.* (1976) and Zen (1986) proposed that strongly peraluminous granites can be formed from crystal fractionation of an I-type granitic magma. The separation of amphibole and pyroxene, which have A/CNK ratios less than 1.0, would increase the A/CNK ratio of residual melt and result in the formation of strongly peraluminous granite. The third point of view raised the possibility that the high A/CNK ratio originated from contamination of the surrounding sedimentary rocks (Ugidos and Recio 1993). Finally, the high A/CNK ratio could also be derived from the alkali loss of end-stage volatile-bearing magmas (Martin and Bowden 1981). Geochemical compositions and mineral textures of the Mengsong two-mica monzogranites in this study indicate that they are of highly fractionated type affinity. We agree with the conclusion of Cawthorn *et al.* (1976) and Zen (1986). The strongly peraluminous feature of the Mengsong pluton can be formed by crystal fractionation of biotite, plagioclase, zircon, monazite, apatite, and allanite. Moreover, the two-mica monzogranites are characterized by high ratios of FeO^{tot}/MgO (10–25.7), therefore, some two-mica monzogranites show A-type characteristics (Figure 6(c)). However, they do not contain the mafic alkaline minerals common to A-type granites, such as arfvedsonite and riebeckite. Furthermore, the significantly low temperatures of two-mica monzogranites (663–692 °C) indicate that they are different from the A-type granite, which are characterized by high temperatures (>900 °C) (Patiño 1997). In addition, the relatively low contents of Ga in all rocks strongly suggest that they do not belong to the A-type (Figure 6(b)). It appears that granites with A-type geochemical characteristics could also be produced from highly differentiated I-type granites (Wu *et al.* 2017). Hence,

we suggest that the Mengsong two-mica monzogranites are highly fractionated granites.

Both the biotite monzogranites and two-mica monzogranites are characterized by negative $\epsilon_{Nd}(t)$ values, and are similar to the Lincang granites and Main Range granitoids on the Malay Peninsula (Figure 8). However, the two-mica monzogranites have lower $(La/Yb)_N$ ratios (1.3–1.7) than those of the Lincang granites (5.9–21.4) (Figure 8), which indicate that the two-mica monzogranites are highly fractionated rocks. In addition, the Mengsong and Lincang granites show negative $\epsilon_{Hf}(t)$ values, while coeval magmatism in Caojian and Manghuai in the southeastern Tibetan Plateau, and Chanthaburi of eastern Thailand, mainly have positive $\epsilon_{Hf}(t)$ values (Figure 9(a)). Most notably, both of them yielded large variations in $^{176}Hf/^{177}Hf$, corresponding to 5–9 ϵ_{Hf} units between zircons of different growth stages within a single rock (Figure 9(b)), and were scattered with no meaningful mean value, suggesting crystallization through continuous hybridization of different sources (Griffin *et al.* 2002; Li *et al.* 2007) or disequilibrium melting in granitic systems (Iles *et al.* 2018). According to variably negative $\epsilon_{Nd}(t)$ and $\epsilon_{Hf}(t)$ values of the Lincang granites, Peng *et al.* (2013) and Cong *et al.* (2020) considered that the Lincang granites were derived from partial melting of the lower crust. Moreover, the old crustal residence ages ($T_{DM2} = 1635\text{--}2167$ Ma based on Nd isotopes) of the Lincang and Mengsong granites support this point of view. The Lincang group in the southeastern Tibetan Plateau, consist mainly of high-grade metamorphic rocks and represents the lower crust of the Indochina block (Zhong 1998). Therefore, we

suggest that partial melting of the Lancang group, could have formed the parental magma of the Lincang and Mengsong granites.

5.3. The crystal mush model

The Indochina and Sibumasu blocks collided in the Early Triassic, based on the following evidence. (1) Early Triassic deposition is commonly absent and the pre-Triassic strata are unconformably overlain by the Middle Triassic Shanglan formation in the Changning-Menglian Paleo-Tethys orogenic belt (YBGMR 1990; Zhong 1998). (2) Records of Early Triassic ultra-high-pressure metamorphism have been recognized in the Changning-Menglian suture zone (Zhang *et al.* 1993; Wang *et al.* 2018). (3) The change in geochemistry of volcanics from intermediate in the Permian to felsic in the Middle–Late Triassic in East Malaysia (Metcalf 2013). In this scenario it is difficult to define the Lincang batholith as an arc batholith, as this age relationship implies it is likely post-collisional. Therefore, post-collisional extension is the most feasible mechanism for the generation of the Middle to Late Triassic Lincang batholith. The mafic magma would formed by mantle upwelling in a post-collisional extension setting. And then the mafic magma rise into the lower crust, where they further induced large-scale crustal melting and silicic magma formation in the Middle to Late Triassic. The hypothesis of mantle upwelling can account for the Triassic granitoids with positive $\epsilon_{Hf}(t)$ values in Paleo-Tethys orogenic

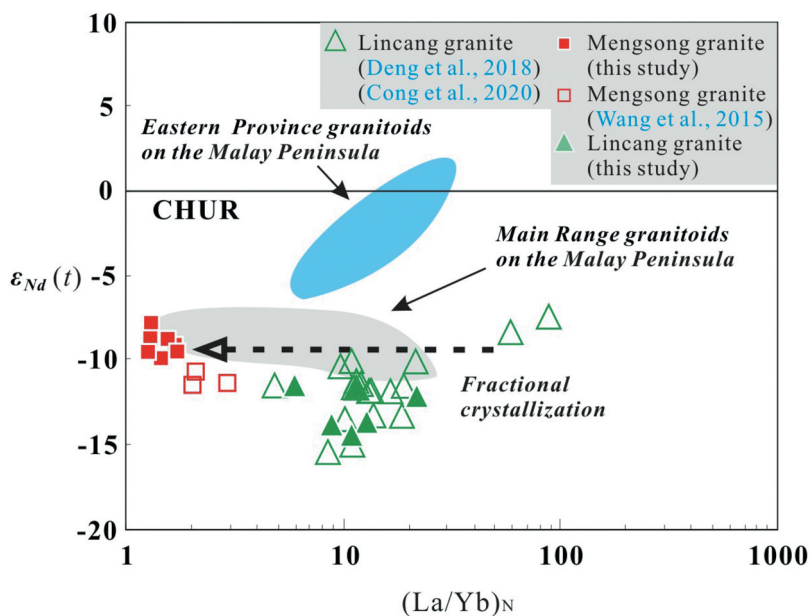


Figure 8. Nd isotope composition of the Lincang and Mengsong granites in the southeastern Tibetan Plateau. Data sources: (1) Eastern and Main Range province granitoids of Malay Peninsula: Ng *et al.* (2015); (2) Lincang granites: Deng *et al.* (2018), Cong *et al.* (2020); this study; (3) Mengsong granites: Wang *et al.* (2015); this study.

belt of Thailand (Wang *et al.* 2016; Qian *et al.* 2017), and the asthenospheric mantle geochemical signature in the Xiaodingxi basalts (Wang *et al.* 2010) and Caojian mafic dikes (Liao *et al.* 2013) in the southeastern Tibetan Plateau. After that, buoyant silicic magmas rised from their deep source regions into the upper crust and formed magma reservoirs.

Many lines of evidence suggest magma reservoirs exist as high-crystallinity ('crystal mush') bodies in the upper crust (Castro 2013; Lipman and Bachmann 2015; Bachmann and Huber 2016). It suggests that felsic volcanic rocks or highly fractionated granites could be seen as

melts expelled from the crystal mush, which later crystallized to form unfractionated granites (Miller and Miller 2002; Bachmann and Bergantz 2004; Hildreth 2004; Bachmann *et al.* 2007). In the crystal mush model (Figure 12), rising basaltic melts would mix efficiently with crystal mush zone, thereby increasing temperatures and melt proportion in the mush body. Geologically, the Late Triassic Xiaodingxi basalts are major components of the Changning-Menglian Paleo-Tethys orogenic belt (Wang *et al.* 2010), and the Middle Triassic Manghuai Formation is dominated by rhyolites with thin interbedded basaltic layers (Peng *et al.* 2013), providing direct

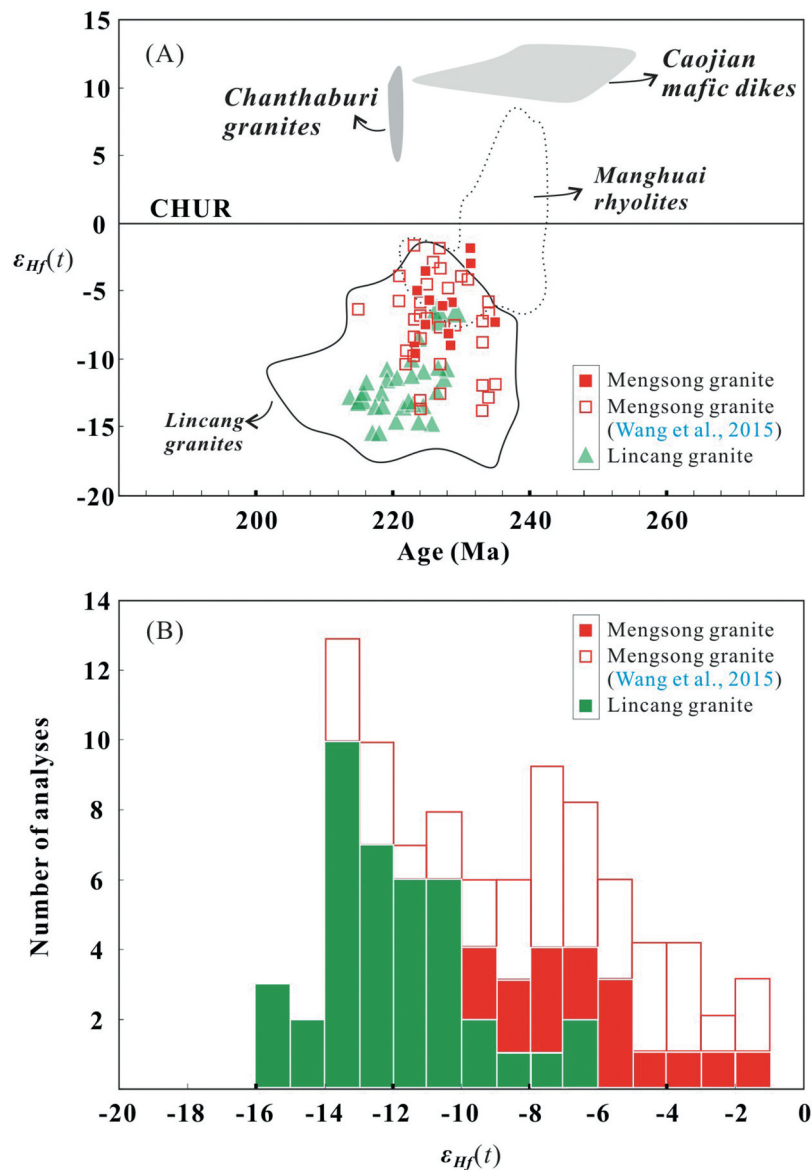


Figure 9. (a) $\epsilon_{Hf}(t)$ of the zircons from the Lincang granites (after Kong *et al.* 2012; Nie *et al.* 2012; Dong *et al.* 2013; Zhao *et al.* 2018; this study), Mengsong granites (Wang *et al.* 2015; this study), Caojian mafic dikes (after Liao *et al.* 2013), Manghuai rhyolites (after Wei *et al.* 2016), and Chanthaburi granites (after Wang *et al.* 2016), plotted against the crystallization age of the zircons. (b) Comparison of $\epsilon_{Hf}(t)$ values between the Lincang and Mengsong granites, showing that the Lincang and Mengsong granites have negative $\epsilon_{Hf}(t)$ values and that Mengsong granites have higher $\epsilon_{Hf}(t)$ values than those of the Lincang granites.

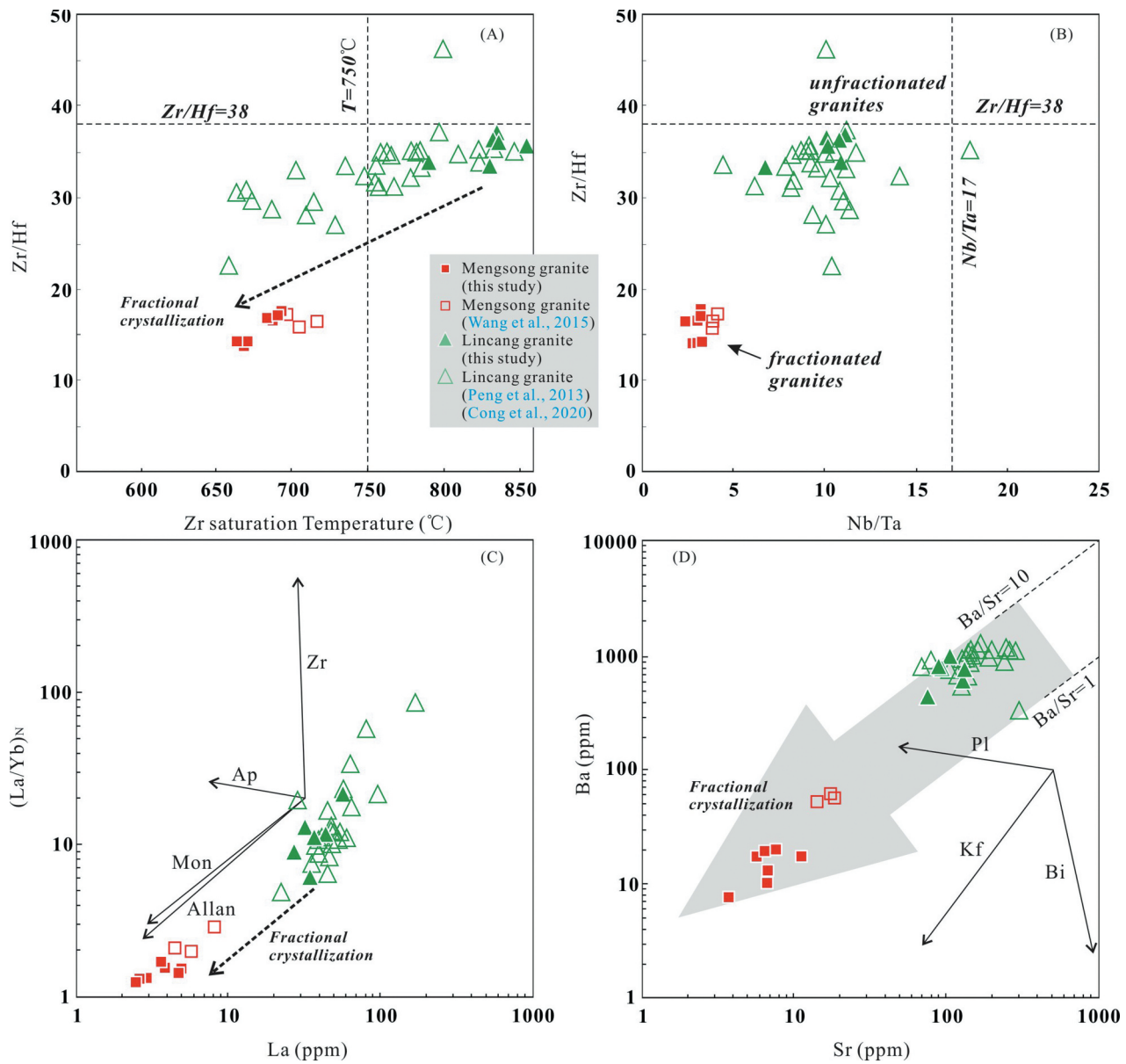


Figure 10. (a) Diagram of Zr/Hf vs. Zr saturation temperature (c), and (b) Diagram of Zr/Hf vs. Nb/Ta, showing that fractionation of zircon played a role in the generation of Mengsong granites. (c) (La/Yb)_N vs. La diagram showing the change in REE patterns caused by separation of accessory minerals, especially allanite and monazite. (d) Ba vs. Sr diagram showing that fractionation of alkali-feldspar, or plagioclase and biotite together, played an important role in differentiation. Data sources: (1) Lincang granites: Dong *et al.* (2013), Cong *et al.* (2020); this study; (2) Mengsong granites: Wang *et al.* (2015); this study. (3) Manghuai rhyolites: Cong *et al.* (2020).

evidence for open-system mafic recharge into the crystal mush. Such processes would permit assembly of a melt-rich zone at the core of the mush body, then the fractionated felsic melt move upward and finally erupt to form the Manghuai rhyolites during the middle Triassic (Cong *et al.* 2020). The Mengsong two-mica monzogranites as intrusive parts of fractionated melts were formed by later crystallization events from the crystal mush reservoirs during the Late Triassic. The Lincang biotite monzogranites were complementary residual of the Manghuai rhyolites and Mengsong two-mica monzogranites.

6. Conclusions

1. The coeval Lincang and Mengsong granites were formed in a post-collisional extension setting during the Middle to Late Triassic, and they are genetically related. Geochemical relationships and mineral textures indicate that two-mica monzogranites are highly fractionated granites, and that the biotite monzogranites are of unfractionated type affinity. Partial melting of the Lincang group could have formed the parental magma of the Lincang and Mengsong granites. The strongly

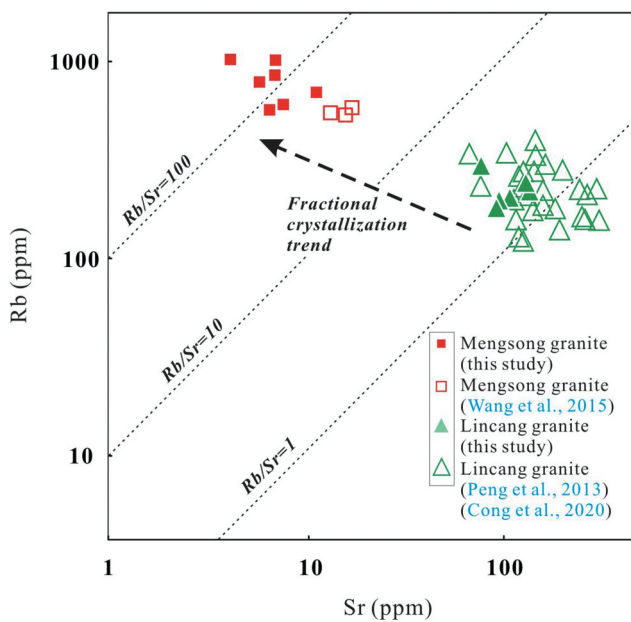


Figure 11. (a) Rb vs. Sr content for the Lincang and Mengsong granites from the southeastern Tibetan Plateau, showing that Mengsong granites record a strong crystal fractionation signature of higher Rb/Sr ratios than those of the Lincang granites. The change in Rb/Sr ratios caused by separation of feldspar. Data sources: (1) Lincang granites: Dong *et al.* (2013), Cong *et al.* (2020); this study; (2) Mengsong granites: Wang *et al.* (2015); this study.

peraluminous feature of the Mengsong pluton can be formed by crystal fractionation.

2. In the crystal mush model, the crystal mush reservoirs were reactivated by new input of mafic magmas, then the highly fractionated felsic melts moved upward and the Mengsong two-mica monzogranites finally formed in the Late Triassic, leaving the Lincang biotite monzogranites as complementary residual.

Acknowledgments

Yue-Heng Yang, Ping Xiao and Lei Xu are gratefully thanked for instrument analyses.

Disclosure statement

No potential conflict of interest was reported by the authors.

Funding

This study was supported by the National Nature Science Foundation of China (project No. 41888101), Science and Technology Foundation of Guizhou Province (project No. [2011]2360) and China Geological Survey (project No. DD20190053).

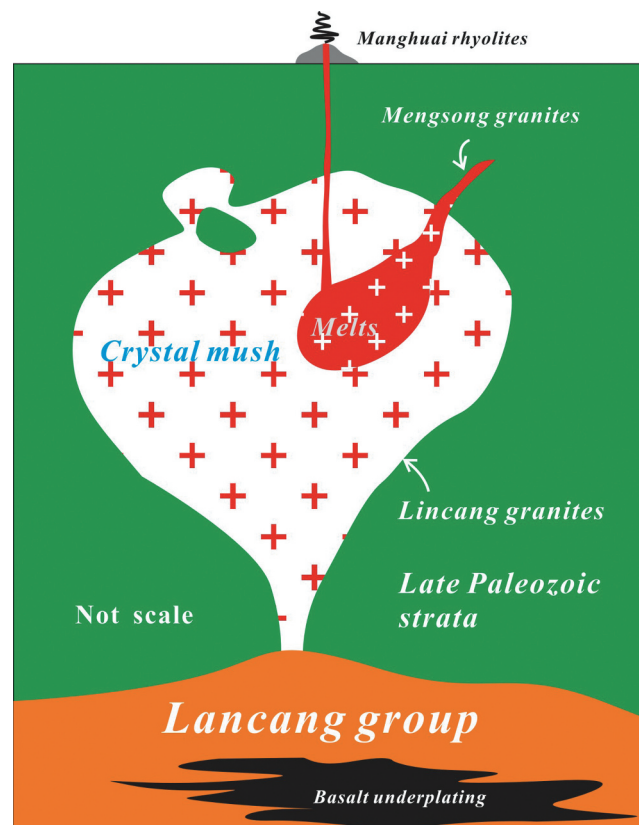


Figure 12. The crystal mush model of the Lincang and Mengsong granites from the southeastern Tibetan Plateau, showing the genetic relationship of the Lincang granites and Mengsong granites (modified from Bachmann and Bergantz 2008; Castro 2013; Cong *et al.* 2020). The mafic magma would formed by mantle upwelling in a post-collisional extension setting during the Middle to Late Triassic. And then the mafic magma rise into the Lancang group, where they further induced large-scale crustal melting and silicic magma formation. In the crystal mush model, rising basaltic melts would mix efficiently with crystal mush zone, thereby increasing temperatures and melt proportion in the mush body. Such processes would permit assembly of a melt-rich zone at the core of the mush body, then the fractionated felsic melt move upward and finally erupt to form the Manghuai rhyolites during the middle Triassic. The Mengsong two-mica monzogranites as intrusive parts of fractionated melts were formed by later crystallization events from the crystal mush reservoirs during the Late Triassic. The Lincang biotite monzogranites were complementary residual of the Manghuai rhyolites and Mengsong two-mica monzogranites.

References

- Bachmann, O., and Bergantz, G.W., 2004, On the origin of crystal-poor rhyolites: Extracted from batholithic crystal mushes: *Journal of Petrology*, v. 45, p. 1565–1582. doi:10.1093/petrology/egh019.
- Bachmann, O., and Bergantz, G.W., 2008, The magma reservoirs that feed supereruptions: *Elements*, v. 4, p. 17–21. doi:10.2113/GSELEMENTS.4.1.17.

- Bachmann, O., and Huber, C., 2016, Silicic magma reservoirs in the Earth's crust: *American Mineralogist*, v. 101, p. 2377–2404. doi:10.2138/am-2016-5675.
- Bachmann, O., Miller, C.F., and de Silva, S.L., 2007, The volcanic-plutonic connection as a stage for understanding crustal magmatism: *Journal of Volcanology and Geothermal Research*, v. 167, p. 1–23. doi:10.1016/j.jvolgeores.2007.08.002.
- Bouvier, A., Vervoort, J.D., and Patchett, P.J., 2008, The Lu-Hf and Sm-Nd isotopic composition of CHUR: Constraints from unequilibrated chondrites and implications for the bulk composition of terrestrial planets: *Earth and Planetary Science Letters*, v. 273, p. 48–57. doi:10.1016/j.epsl.2008.06.010.
- Castro, A., 2013, Tonalite-granodiorite suites as cotectic systems: A review of experimental studies with applications to granitoid petrogenesis: *Earth-Science Reviews*, v. 124, p. 68–95. doi:10.1016/j.earscirev.2013.05.006.
- Cawthorn, R.G., Strong, D.F., and Brown, P.A., 1976, Origin of corundum-normative intrusive and extrusive magmas: *Nature*, v. 259, p. 102–104. doi:10.1038/259102a0.
- Chappell, B.W., Bryant, C.J., and Wyborn, D., 2012, Peraluminous I-type granites: *Lithos*, v. 153, p. 142–153. doi:10.1016/j.lithos.2012.07.008.
- Chappell, B.W., and White, A.J.R., 1992, I- and S-type granites in the Lachlan Fold Belt: *Transactions of the Royal Society of Edinburgh Earth*, v. 83, p. 1–26.
- Chappell, B.W., and Wyborn, D., 2004, Cumulate and cumulative granites and associated rocks: *Resource Geology*, v. 54, p. 227–240. doi:10.1111/j.1751-3928.2004.tb00204.x.
- Charusiri, P., Clark, A.H., Farrar, E., Archibald, D., and Charusiri, B., 1993, Granite belts in Thailand: Evidence from the $^{40}\text{Ar}/^{39}\text{Ar}$ geochronological and geological syntheses: *Journal of Southeast Asian Earth Sciences*, v. 8, no. 1–4, p. 127–136. doi:10.1016/0743-9547(93)90014-G.
- Chen, F., Li, X.H., Wang, X.L., Li, Q.L., and Siebel, W., 2007, Zircon age and Nd-Hf isotopic composition of the Yunnan Tethyan belt, southwestern China: *International Journal of Earth Sciences*, v. 96, p. 1179–1194. doi:10.1007/s00531-006-0146-y.
- Clemens, J.D., and Stevens, G., 2012, What controls chemical variation in granitic magmas?: *Lithos*, v. 134–135, p. 317–329. doi:10.1016/j.lithos.2012.01.001.
- Cobbing, E.J., Mallick, D.I.J., Pitfield, P.E.J., and Teoh, L.H., 1986, The granites of the Southeast Asia Tin Belt: *Journal of the Geological Society*, v. 143, p. 537–550. doi:10.1144/gsjgs.143.3.0537.
- Cong, F., Wu, F.Y., Li, W.C., Mou, C.L., Huang, X.M., Wang, B.D., Hu, F.Y., and Peng, Z.M., 2020, Origin of the Triassic Lincang granites in the southeastern Tibetan Plateau: Crystallization from crystal mush: *Lithos*, v. 360–361, p. 105452. doi:10.1016/j.lithos.2020.105452.
- Deng, J., Wang, C.M., Zi, J.W., Xia, R., and Li, Q., 2018, Constraining subduction-collision processes of the Paleo-Tethys along the Changning-Menglian Suture: New zircon U-Pb ages and Sr-Nd-Pb-Hf-O isotopes of the Lincang Batholith: *Gondwana Research*, v. 62, p. 75–92. doi:10.1016/j.gr.2017.10.008.
- Dong, G.C., Mo, X.X., Zhao, Z.D., Zhu, D.C., Goodman, R.C., Kong, H.L., and Wang, S., 2013, Zircon U-Pb dating and the petrological and geochemical constraints on Lincang granite in Western Yunnan, China: Implications for the closure of the Paleo-Tethys Ocean: *Journal of Asian Earth Sciences*, v. 62, p. 282–294. doi:10.1016/j.jseaeas.2012.10.003.
- Fan, W.M., Peng, T.P., and Wang, Y.J., 2009, Triassic magmatism in the southern Lancangjiang zone, southwestern China and its constraints on the tectonic evolution of Paleo-Tethys: *Frontiers in Earth Science*, v. 16, no. 6, p. 291–302. (in Chinese).
- Frost, B.R., Barnes, C.G., Collins, W.J., Arculus, R.J., Ellis, D.J., and Frost, C.D., 2001, A geochemical classification for granitic rocks: *Journal of Petrology*, v. 42, no. 11, p. 2033–2048. doi:10.1093/petrology/42.11.2033.
- Gardiner, N.J., Searle, M.P., Morley, C.K., Whitehouse, M.P., Spencer, C.J., and Robb, L.J., 2016, The closure of Palaeo-Tethys in Eastern Myanmar and Northern Thailand: New insights from zircon U-Pb and Hf isotope data: *Gondwana Research*, v. 39, p. 401–422. doi:10.1016/j.gr.2015.03.001.
- Glazner, A.F., and Johnson, B.R., 2013, Late crystallization of K-feldspar and the paradox of megacrystic granites: *Contributions to Mineralogy and Petrology*, v. 166, p. 777–799. doi:10.1007/s00410-013-0914-1.
- Griffin, W.L., Pearson, N.J., Belousova, E., Jackson, S.E., van Acherbergh, E., O'Reilly, S.Y., and Shee, S.R., 2000, The Hf isotope composition of cratonic mantle: LAM-MC-ICPMS analysis of zircon megacrysts in kimberlites: *Geochimica et Cosmochimica Acta*, v. 64, p. 133–147. doi:10.1016/S0016-7037(99)00343-9.
- Griffin, W.L., Wang, X., Jackson, S.E., Pearson, N.J., O'Reilly, S.Y., Xu, X.S., and Zhou, X.M., 2002, Zircon chemistry and magma mixing, SE China: In-situ analysis of Hf isotopes, Tonglu and Pingtan igneous complexes: *Lithos*, v. 61, p. 237–269. doi:10.1016/S0024-4937(02)00082-8.
- Hennig, D., Lehmann, B., Frei, D., Belyatsky, B., Zhao, X.F., Cabral, A.R., Zeng, P.S., Zhou, M.F., and Schmidt, K., 2009, Early Permian seafloor to continental arc magmatism in the eastern Paleo-Tethys: U-Pb age and Nd-Sr isotope data from the southern Lancangjiang zone, Yunnan, China: *Lithos*, v. 113, p. 408–422. doi:10.1016/j.lithos.2009.04.031.
- Hildreth, W., 2004, Volcanological perspectives on Long Valley, Mammoth Mountain, and Mono Craters: Several contiguous but discrete systems: *Journal of Volcanology and Geothermal Research*, v. 136, no. 3–4, p. 169–198. doi:10.1016/j.jvolgeores.2004.05.019.
- Hutchison, C.S., 1977, Granite emplacement and tectonic subdivision in Peninsular Malaysia: *Bulletin of the Geological Society of Malaysia*, v. 9, p. 187–207. doi:10.7186/bgsm09197714.
- Iles, K.A., Hergt, J.M., and Woodhead, J.D., 2018, Modelling isotopic responses to disequilibrium melting in granitic systems: *Journal of Petrology*, v. 59, no. 1, p. 87–114. doi:10.1093/petrology/egy019.
- Jahn, B.M., Wu, F.Y., Capdevila, R., Martineau, F., Zhao, Z.H., and Wang, Y.X., 2001, Highly evolved juvenile granites with tetrad REE patterns: The Woduhe and Baerzhe granites from the Great Xing'an Mountains in NE China: *Lithos*, v. 59, p. 171–198. doi:10.1016/S0024-4937(01)00066-4.
- Jian, P., Liu, D., Kröner, A., Zhang, Q., Wang, Y., Sun, X., and Zhang, W., 2009, Devonian to Permian plate tectonic cycle of the Paleo-Tethys Orogen in southwest China (II), insights from zircon ages of ophiolites, arc/back-arc assemblages and within-plate igneous rocks and generation of the

- Emeishan CFB province: *Lithos*, v. 113, p. 767–784. doi:10.1016/j.lithos.2009.04.006.
- Kong, H.L., Dong, G.C., Mo, X.X., Zhao, Z.D., Zhu, D.C., Wang, S., Li, R., and Wang, Q.L., 2012, Petrogenesis of Lincang granites in Sanjiang area of western Yunnan Province: Constraints from geochemistry, zircon U-Pb geochronology and Hf isotope: *Acta Petrologica Sinica*, v. 28, no. 5, p. 1438–1452. (in Chinese).
- Li, X.H., Li, Z.X., Li, W.X., Liu, Y., Yuan, C., Wei, G.J., and Qi, C.S., 2007, U-Pb zircon, geochemical and Sr-Nd-Hf isotopic constraints on age and origin of Jurassic I- and A-type granites from central Guangdong, SE China: A major igneous event in response to foundering of a subducted flat-slab?: *Lithos*, v. 96, p. 186–204. doi:10.1016/j.lithos.2006.09.018.
- Li, X.L., 1996, Basic characteristics and formation structural environment of Lincang composite granite batholith: *Geology in Yunnan*, v. 15, no. 1, p. 1–18. (in Chinese).
- Liao, S.Y., Yin, F.G., Sun, Z.M., Wang, D.B., Tang, Y., and Sun, J., 2013, Early Middle Triassic mafic dikes from the Baoshan subterranean, western Yunnan: Implications for the tectonic evolution of the Palaeo-Tethys in Southeast Asia: *International Geology Review*, v. 55, no. 8, p. 976–993. doi:10.1080/00206814.2012.758354.
- Lipman, P.W., and Bachmann, O., 2015, Ignimbrites to batholiths: Integrating perspectives from geological, geophysical, and geochronological data: *Geosphere*, v. 11, no. 3, p. 705–743.
- Liu, Y.S., Hu, Z.C., Gao, S., Günther, D., Xu, J., Gao, C.G., and Chen, H.H., 2008, In situ analysis of major and trace elements of anhydrous minerals by LA-ICP-MS without applying an internal standard: *Chemical Geology*, v. 257, no. 1–2, p. 34–43. doi:10.1016/j.chemgeo.2008.08.004.
- Martin, R.F., and Bowden, P., 1981, Peraluminous granites produced by rock-fluid interaction in the Ririwai nonorogenic ring-complex, Nigeria: *Mineralogical evidence: The Canadian Mineralogist*, v. 19, p. 65–82.
- Metcalf, I., 2011, Tectonic framework and Phanerozoic evolution of Sundaland: *Gondwana Research*, v. 19, no. 1, p. 3–21. doi:10.1016/j.gr.2010.02.016.
- Metcalf, I., 2013, Tectonic evolution of the Malay Peninsula: *Journal of Asian Earth Sciences*, v. 76, p. 195–213. doi:10.1016/j.jseaes.2012.12.011.
- Miller, C.F., and Miller, J.S., 2002, Contrasting stratified plutons exposed in tilt blocks, Eldorado Mountains, Colorado River Rift, NV, USA: *Lithos*, v. 61, no. 3–4, p. 209–224. doi:10.1016/S0024-4937(02)00080-4.
- Mitchell, A.H.G., 1977, Tectonic settings for the emplacement of the Southeast Asian tin granites: *Bulletin of the Geological Society of Malaysia*, v. 9, p. 123–140. doi:10.7186/bgsm09197710.
- Morel, M.L.A., Nebel, O., Nebel-Jacobsen, Y.J., Miller, J.S., and Vroon, P.Z., 2008, Hafnium isotope characterization of the GJ-1 zircon reference material by solution and laser-ablation MC-ICPMS: *Chemical Geology*, v. 255, p. 231–235. doi:10.1016/j.chemgeo.2008.06.040.
- Ng, S.W.P., Chung, S.L., Robb, L.J., Searle, M.P., Ghani, A.A., Whitehouse, M.J., Oliver, G.J.H., Sone, M., Gardiner, N.J., and Roselee, M.H., 2015, Petrogenesis of Malaysian granitoids in the Southeast Asian tin belt: Part 1. Geochemical and Sr-Nd isotopic characteristics: *Geological Society of America Bulletin*. doi:10.1130/B31213.1.
- Nie, F., Dong, G.C., Mo, X.X., Zhu, D.C., Dong, M.L., and Wang, X., 2012, Geochemistry, zircon U-Pb chronology of the Triassic granites in the Changning-Menglian suture zone and their implications: *Acta Petrologica Sinica*, v. 28, no. 5, p. 1465–1476. (in Chinese).
- Patiño, D.A.E., 1997, Generation of metaluminous A-type granites by low-pressure melting of calc-alkaline granitoids: *Geology*, v. 25, no. 8, p. 743–746. doi:10.1130/0091-7613-(1997)025<0743:GOMATG>2.3.CO;2.
- Patiño, D.A.E., 1999, What do experiments tell us about the relative contributions of crust and mantle to the origin of granitic magmas? *Geol: Geological Society, London, Special Publications*, v. 168, no. 1, p. 55–75. doi:10.1144/GSL.SP.1999.168.01.05.
- Peng, T.P., Wang, Y.J., Fan, W.M., Liu, D.Y., Shi, Y.R., and Miao, L. C., 2006, SHRIMP zircon U-Pb geochronology of early Mesozoic felsic igneous rocks from the southern Lancangjiang and its tectonic implications: *Science in China Series D:Earth Sciences*, v. 49, no. 10, p. 1032–1042. doi:10.1007/s11430-006-1032-y
- Peng, T.P., Wilde, S.A., Wang, Y.J., Fan, W.M., and Peng, B.X., 2013, Mid-Triassic felsic igneous rocks from the southern Lancangjiang Zone, SW China: Petrogenesis and implications for the evolution of Pale-Tethys: *Lithos*, v. 168–169, p. 15–32. doi:10.1016/j.lithos.2013.01.015.
- Pitcher, W.S., 1982, Granite type and tectonic environment, *in* Hsu, K.J., ed., *Mountain Building Processes*: London, Academic Press, p.19–40.
- Qian, X., Feng, Q.L., Wang, Y.J., Zhao, T.Y., Zi, J.W., Udchachon, M., and Wang, Y.K., 2017, Late Triassic post-collisional granites related to Paleotethyan evolution in SE Thailand: Geochronological and geochemical constraints: *Lithos*, v. 286–287, p. 440–453. doi:10.1016/j.lithos.2017.06.026.
- Söderlund, U., Patchett, P.J., Vervoort, J.D., and Isachsen, C.E., 2004, The ¹⁷⁶Lu decay constant determined by Lu-Hf and U-Pb isotope systematics of Precambrian mafic intrusions: *Earth and Planetary Science Letters*, v. 219, p. 311–324. doi:10.1016/S0012-821X(04)00012-3.
- Sone, M., and Metcalfe, I., 2008, Parallel Tethyan sutures in mainland Southeast Asia: New insights for Palaeo-Tethys closure and implications for the Indosinian orogeny: *Comptes Rendus Geoscience*, v. 340, no. 2–3, p. 166–179. doi:10.1016/j.crte.2007.09.008.
- Sun, S.S., and McDonough, W.F., 1989, Chemical and isotopic systematics of oceanic basalts: Implications for mantle composition and processes, *in* Saunders, A.D., and Norry, M.J., eds., *Magmatism in the ocean basins*, Volume Vol. 42: *Geo. Soc. London Special Pub*, p.313–345.
- Sun, Z.B., Hu, S.B., Zhou, K., Wang, Y.X., Liu, G.C., Wu, J.L., and Zhao, J.T., 2018, Zircon U-Pb age, Hf isotopic composition of the Bulang-shan Ordovician granite in the Menghai area, southwestern Yunnan Province, and its tectonic significance: *Geological Bulletin of China*, v. 37, no. 11, p. 2044–2054. (in Chinese).
- Sylvester, P.J., 1998, Post-collisional strongly peraluminous granites: *Lithos*, v. 45, p. 29–44. doi:10.1016/S0024-4937(98)00024-3.
- Ugidos, J.M., and Recio, C., 1993, Origin of cordierite-bearing granites by assimilation in the Central Iberian Massif (CIM), Spain: *Chemical Geology*, v. 103, p. 27–43. doi:10.1016/0009-2541(93)90289-U.

- Wang, C.M., Deng, J., Santosh, M., Lu, Y.J., McCuaig, T.C., Carranza, E.J.M., and Wang, Q.F., 2015, Age and origin of the Bulangshan and Mengsong granitoids and their significance for post-collisional tectonics in the Changning-Menglian Paleo-Tethys Orogen: *Journal of Asian Earth Sciences*, v. 113, p. 656–676.
- Wang, F., Liu, F.L., Ji, L., and Liu, L.S., 2017, LA-ICP-MS U-Pb dating of detrital zircon from low-grade metamorphic rocks of the Lancang Group in the Lancangjiang Complex and its tectonic implications: *Acta Petrologica Sinica*, v. 33, no. 9, p. 2975–2985. (in Chinese).
- Wang, F., Liu, F.L., Liu, P.H., Shi, J.R., and Cai, J., 2014, Petrogenesis of Lincang granites in the south of Lancangjiang area: Constrain from geochemistry and zircon U-Pb geochronology: *Acta Petrologica Sinica*, v. 30, no. 10, p. 3034–3050. (in Chinese).
- Wang, H.N., Liu, F.L., Li, J., Sun, Z.B., Ji, L., Tian, Z.H., Liu, L.S., and Santosh, M., 2018, Petrology, geochemistry and P-T-t path of lawsonite-bearing retrograded eclogites in the Changning-Menglian orogenic belt, southeast Tibetan Plateau: *Journal of Metamorphic Geology*. doi:10.1111/jmg.12462.
- Wang, Y.J., He, H.Y., Cawood, P.A., Srithai, B., Feng, Q.L., Fan, W.M., Zhang, Y.Z., and Qian, X., 2016, Geochronological, elemental and Sr-Nd-Hf-O isotopic constraints on the petrogenesis of the Triassic post-collisional granitic rocks in NW Thailand and its Paleotethyan implications: *Lithos*, v. 266–267, p. 264–286. doi:10.1016/j.lithos.2016.09.012.
- Wang, Y.J., Zhang, A.M., Fan, W.M., Peng, T.P., Zhang, F.F., Zhang, Y.H., and Bi, X.W., 2010, Petrogenesis of late Triassic post-collisional basaltic rocks of the Lancangjiang tectonic zone, southwest China, and tectonic implications for the evolution of the eastern Paleotethys: *Geochronological and geochemical constraints: Lithos*, v. 120, no. 3–4, p. 529–546. doi:10.1016/j.lithos.2010.09.012.
- Watson, E.B., and Harrison, T.M., 1983, Zircon saturation revisited: Temperature and composition effects in a variety of crustal magma types: *Earth and Planetary Science Letters*, v. 64, p. 295–304. doi:10.1016/0012-821X(83)90211-X.
- Wei, C., Qi, X.X., Chang, Y.L., Ji, F.B., and Zhang, S.Q., 2016, Identification on Age of Xiaodingxi Formation Volcanic Rocks in Central-Southern Lancangjiang Orogeny and Its Tectonic Implication: *Acta Geologica Sinica*, v. 90, no. 11, p. 3192–3214. (in Chinese).
- Whalen, J.B., Currie, K.L., and Chappell, B.W., 1987, A-type granites: Geochemical characteristics, discrimination and petrogenesis: *Contributions to Mineralogy and Petrology*, v. 95, p. 407–419. doi:10.1007/BF00402202.
- Wu, F.Y., Jahn, B.M., Wilde, S., and Sun, D.Y., 2000, Phanerozoic crustal growth: U-Pb and Sr-Nd isotopic evidence from the granites in northeastern China: *Tectonophysics*, v. 328, p. 89–113. doi:10.1016/S0040-1951(00)00179-7.
- Wu, F.Y., Jahn, B.M., Wilde, S.A., Lo, C.H., Yui, T.F., Lin, Q., Ge, W. C., and Sun, D.Y., 2003, Highly fractionated I-type granites in NE China (I): *Geochronology and petrogenesis: Lithos*, v. 66, p. 241–273. doi:10.1016/S0024-4937(02)00222-0.
- Wu, F.Y., Liu, X.C., Ji, W.Q., Wang, J.M., and Yang, L., 2017, Highly fractionated granites: Recognition and research: *Science China Earth Sciences*, v. 60, no. 7, p. 1201–1219. doi:10.1007/s11430-016-5139-1.
- Wu, F.Y., Liu, X.C., Liu, Z.C., Wang, R.C., Xie, L., Wang, J.M., Ji, W. Q., Yang, L., Liu, C., Khanal, G.P., and He, S.X., 2020, Highly fractionated Himalayan leucogranites and associated rare-metal mineralization: *Lithos*, v. 352–353, p. 105319. doi:10.1016/j.lithos.2019.105319.
- Wu, F.Y., Yang, Y.H., Xie, L.W., Yang, J.H., and Xu, P., 2006, Hf isotopic compositions of the standard zircons and baddeleyites used in U-Pb geochronology: *Chemical Geology*, v. 234, p. 105–126. doi:10.1016/j.chemgeo.2006.05.003.
- YBGMR (Bureau of Geology and Mineral Resources of Yunnan Province), 1980, 1:200000 Regional Geological map of Menghai and Mengma (in Chinese).
- YBGMR (Bureau of Geology and Mineral Resources of Yunnan Province), 1990, Regional Geology of Yunnan Province: Beijing, Geological Publishing House, p. 1–729. (in Chinese).
- Zen, E.A., 1986, Aluminum enrichment in silicate melts by fractional crystallization: Some mineralogic and petrographic constraints: *Journal of Petrology*, v. 27, p. 1095–1117. doi:10.1093/petrology/27.5.1095.
- Zhang, R.Y., Cong, B.L., Maruyama, S., and Liou, J.G., 1993, Metamorphism and tectonic evolution of the Lancang paired metamorphic belts, south-western China: *Journal of Metamorphic Geology*, v. 11, p. 605–619. doi:10.1111/j.1525-1314.1993.tb00175.x.
- Zhao, F., Li, G.J., Zhang, P.F., Wang, C.B., Sun, Z.B., and Tang, X., 2018, Petrogenesis and tectonic implications of the Lincang batholith in the Sanjiang, Southwest China: Constraints by geochemistry, zircon U-Pb chronology and Hf isotope: *Acta Petrologica Sinica*, v. 34, no. 5, p. 1397–1412. (in Chinese).
- Zhong, D.L., 1998, The Paleotethys Orogenic Belt in West of Sichuan and Yunnan: Beijing, Science Publishing House, p. pp. 1–230. (in Chinese).